



# What questions are raised by a video such as this?

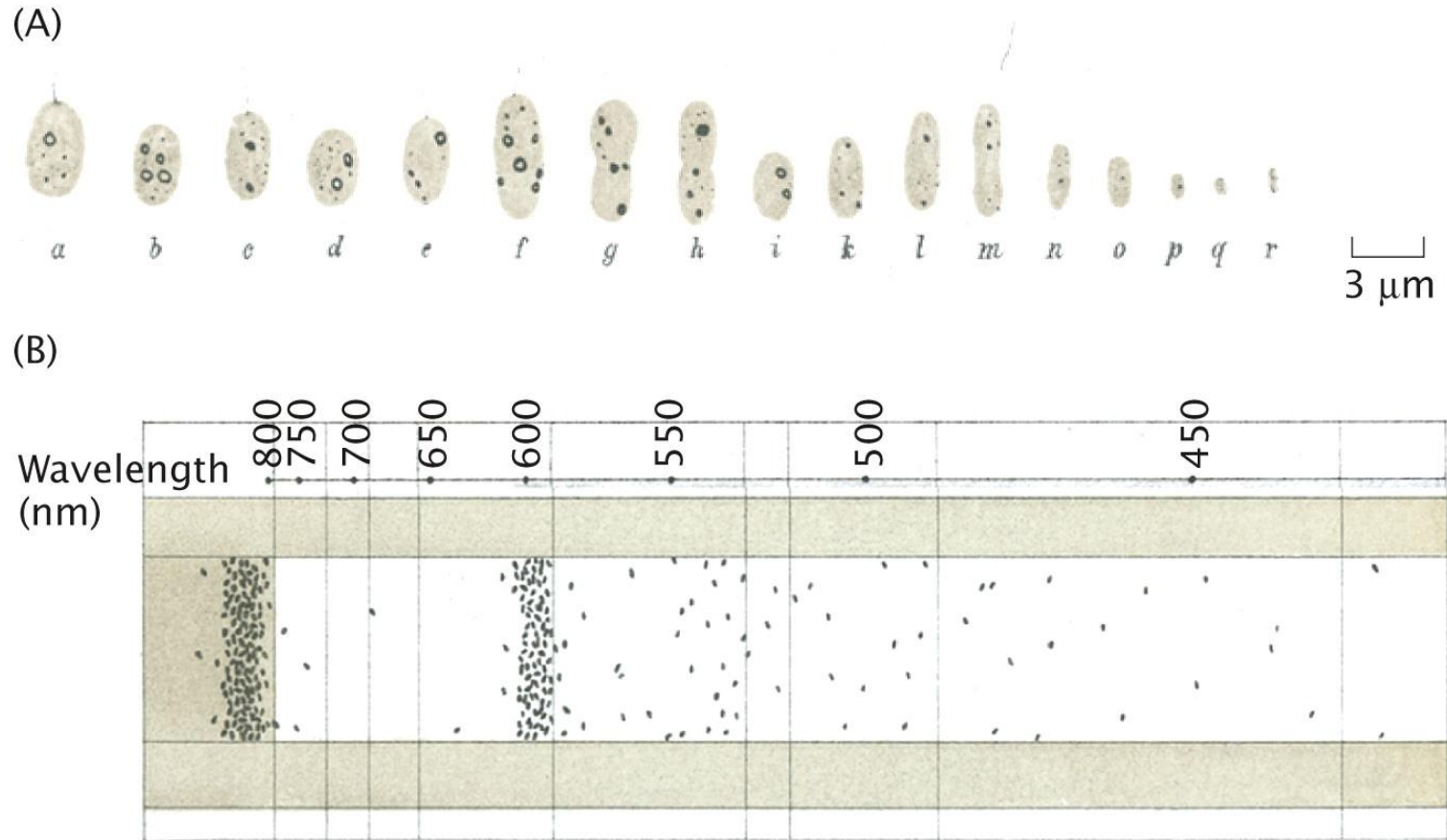


Figure 18.1 Physical Biology of the Cell, 2ed. (© Garland Science 2013)

# Julius Adler studies on chemotaxis

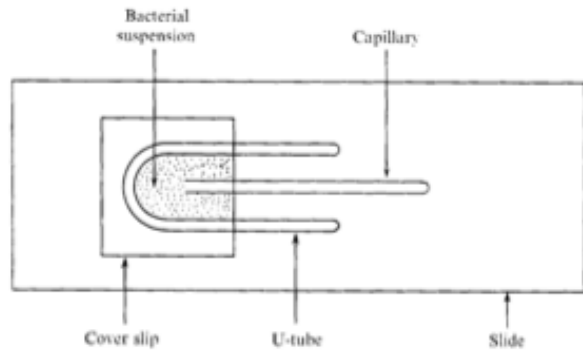


Fig. 1. Apparatus used in the chemotaxis assay. The drawing is to scale except that the capillary is exaggerated.

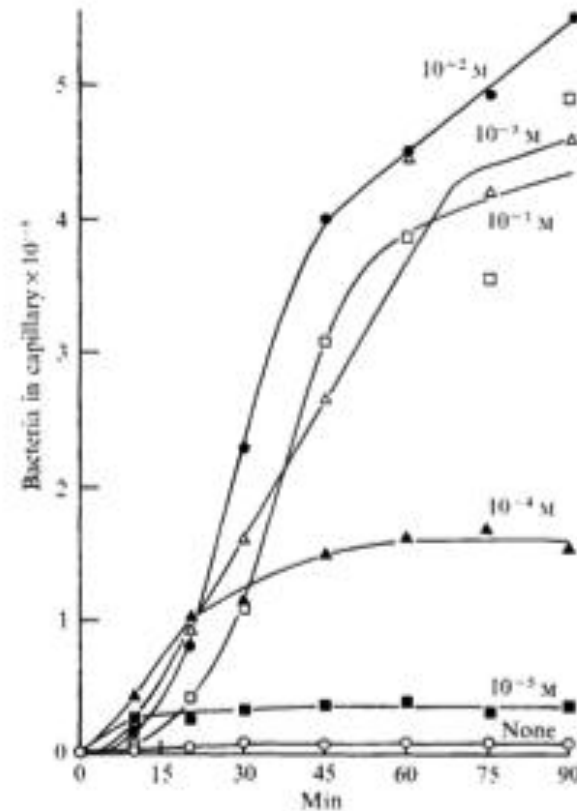


Fig. 2. Rate of accumulation of bacteria in capillaries containing various concentrations of L-aspartate. ○—○, No aspartate; ■—■, 10<sup>-5</sup> M; ▲—▲, 10<sup>-4</sup> M; △—△, 10<sup>-3</sup> M; ●—●, 10<sup>-2</sup> M; □—□, 10<sup>-1</sup> M. Data from two experiments were combined. The experiments were carried out at 30 °C.

*Journal of General Microbiology* (1973), 74,  
77-91 A Method for Measuring Chemotaxis and  
Use of the Method to Determine Optimum  
Conditions for Chemotaxis by *Escherichia coli*  
By J. ADLER

# Bacterial motility in chemotaxis

- We have already seen the strategy of neutrophils for chasing down cellular offenders.
- Bacteria also exhibit motile strategies based upon environmental cues.

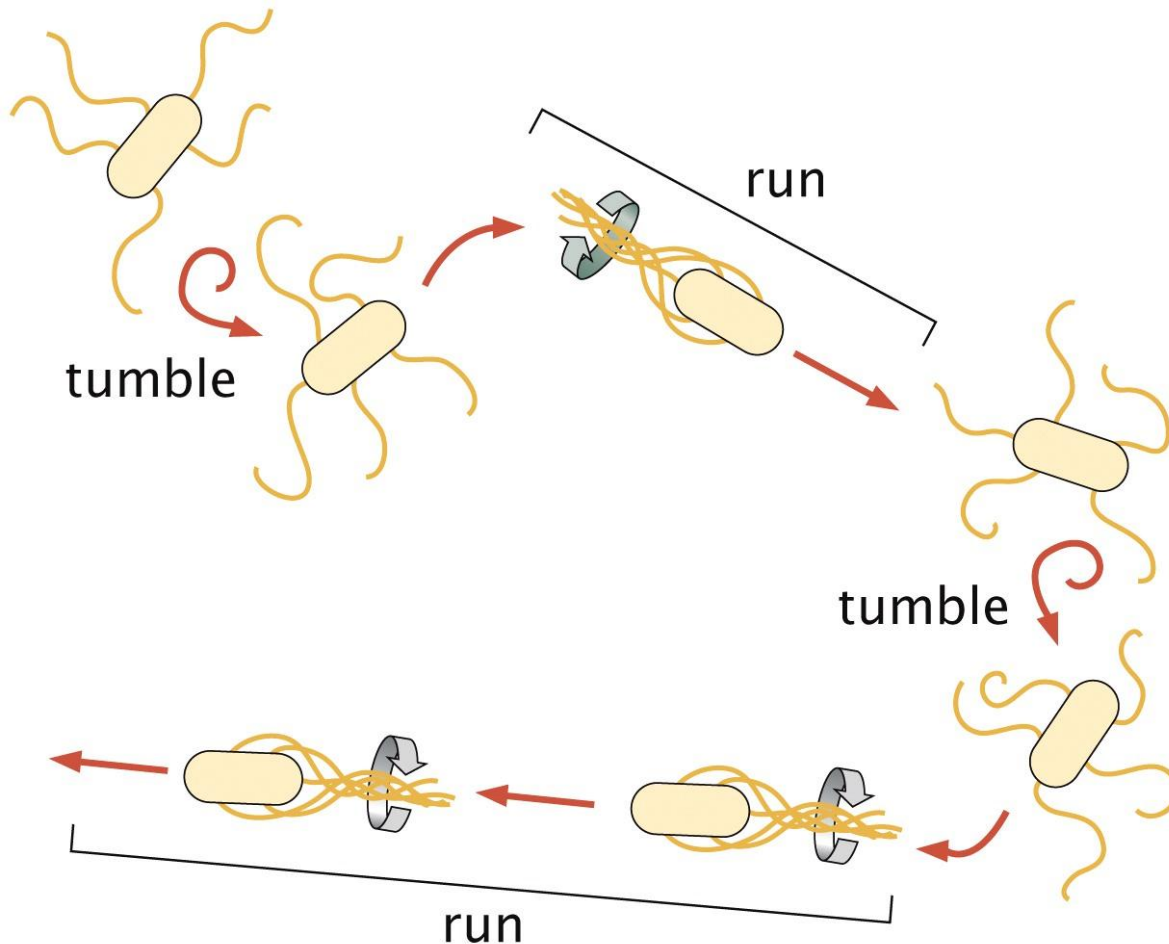
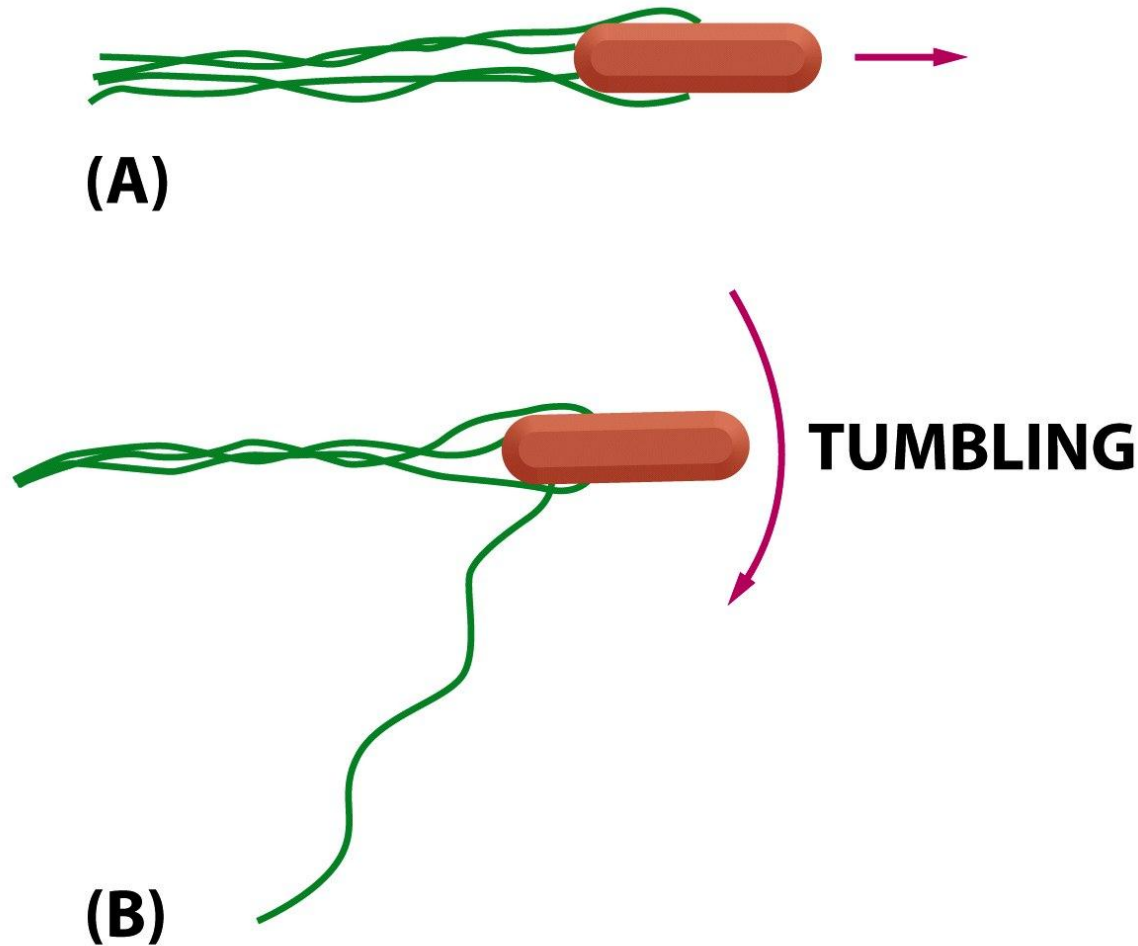


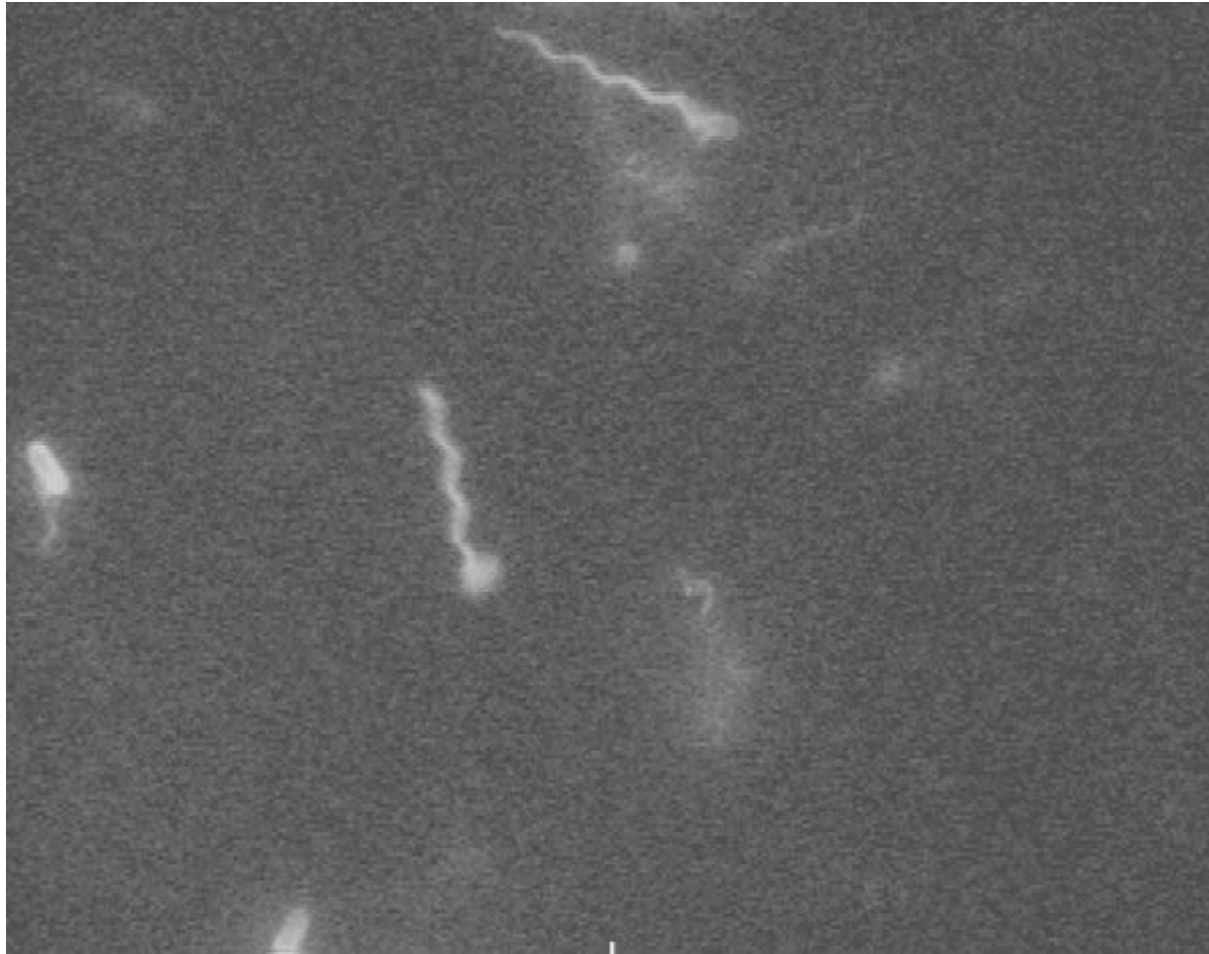
Figure 4.16b Physical Biology of the Cell, 2ed. (© Garland Science 2013)

# *Mechanistic basis of the observed behavior*

- Motion is distinguished by two features – runs and tumbles.



# *Dynamics: Video from Berg and Turner*



# Chemotaxis defined

- The statistics of the motion will change in the presence of a chemical gradient of chemoattractant.

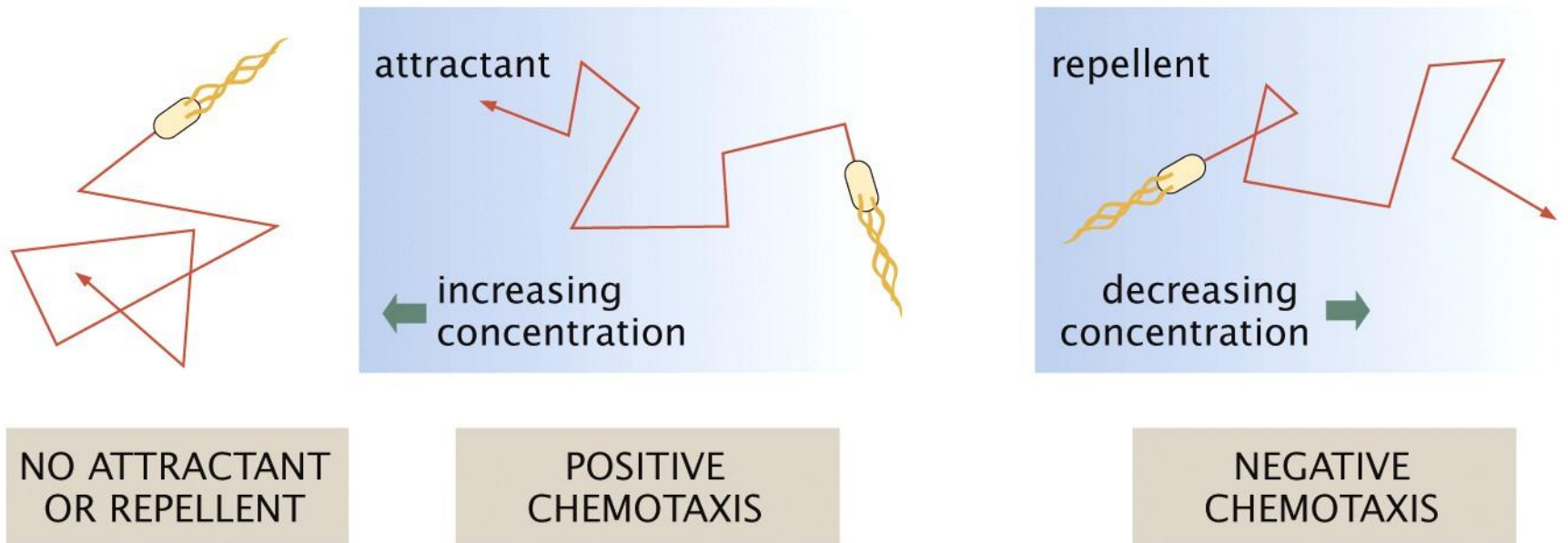


Figure 4.16d Physical Biology of the Cell, 2ed. (© Garland Science 2013)



# Cellular decisions and swimming

- From this kind of data we can extract the statistics of run times and the swimming speed.

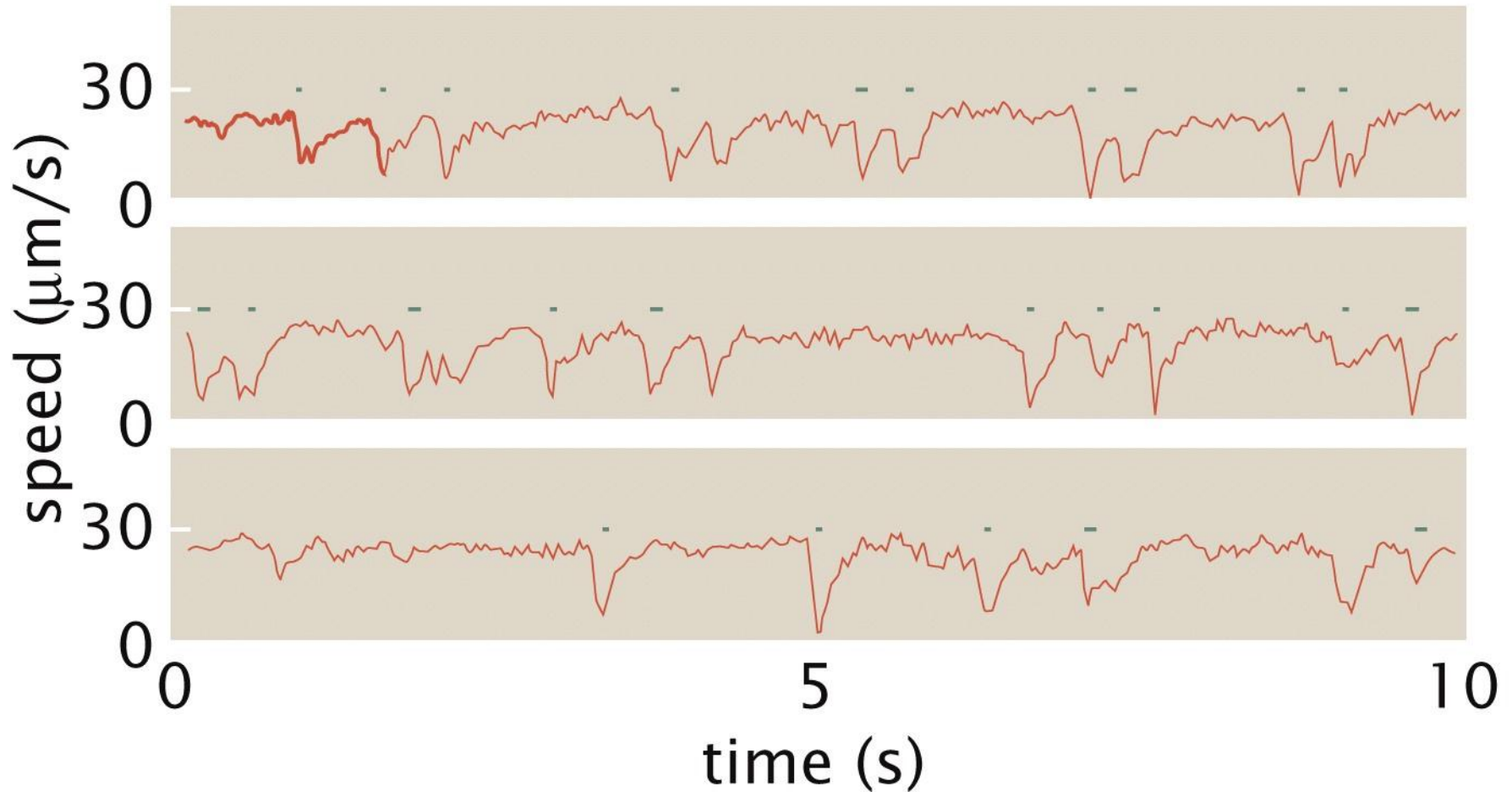


Figure 19.52a Physical Biology of the Cell, 2ed. (© Garland Science 2013)

*adapted from H. C. Berg and D. A. Brown, Nature 239:500, 1972;*



# Cellular decisions and swimming

- We have already seen the strategy of neutrophils for chasing down cellular offenders.
- Bacteria also exhibit motile strategies based upon environmental cues.

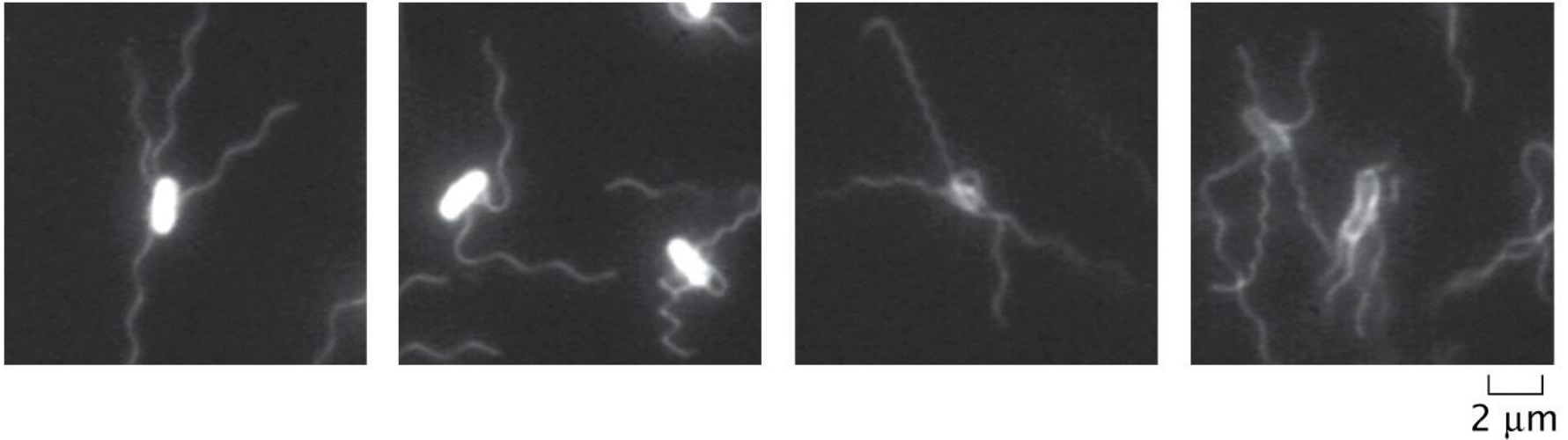


Figure 19.52c *Physical Biology of the Cell*, 2ed. (© Garland Science 2013)

# High-resolution study of chemotaxis

- Hold the bacterium in an optical trap.
- Fluorescently label so that flagellum can be studied over time and then record the dynamics.

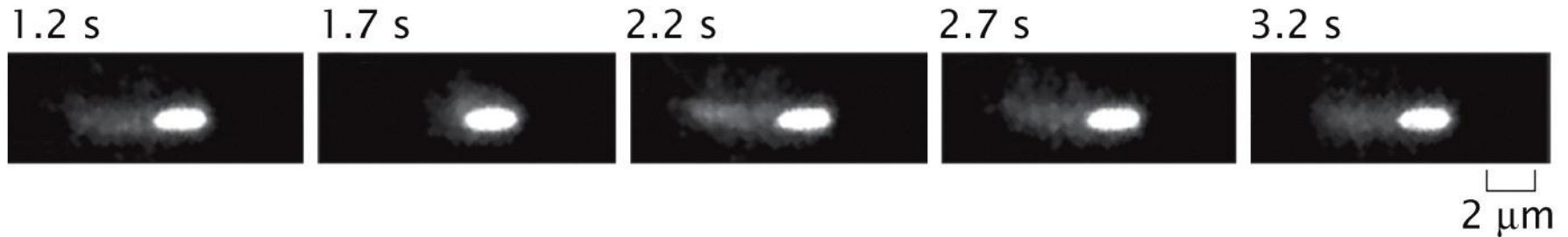


Figure 19.52d Physical Biology of the Cell, 2ed. (© Garland Science 2013)

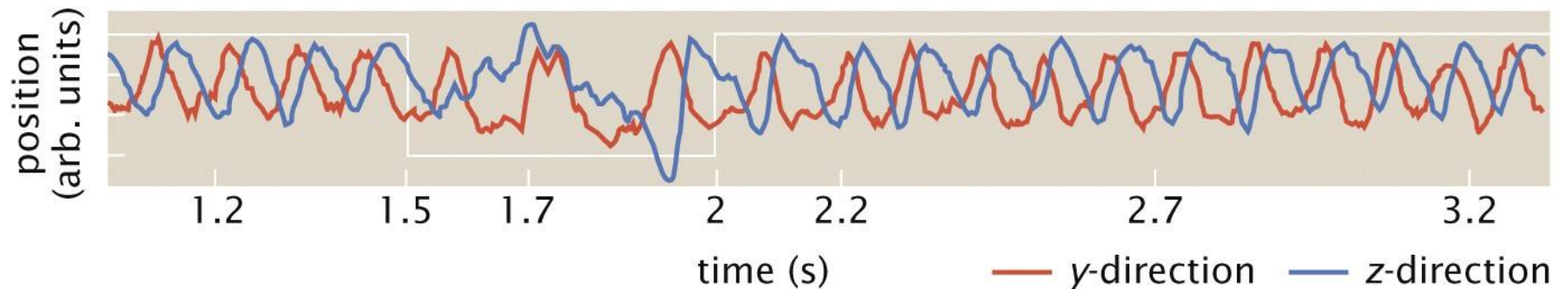


Figure 19.52e Physical Biology of the Cell, 2ed. (© Garland Science 2013)

*adapted from T. L. Min et al., Nat. Methods, 6:831, 2009.)*

# The molecular machines responsible for the motion

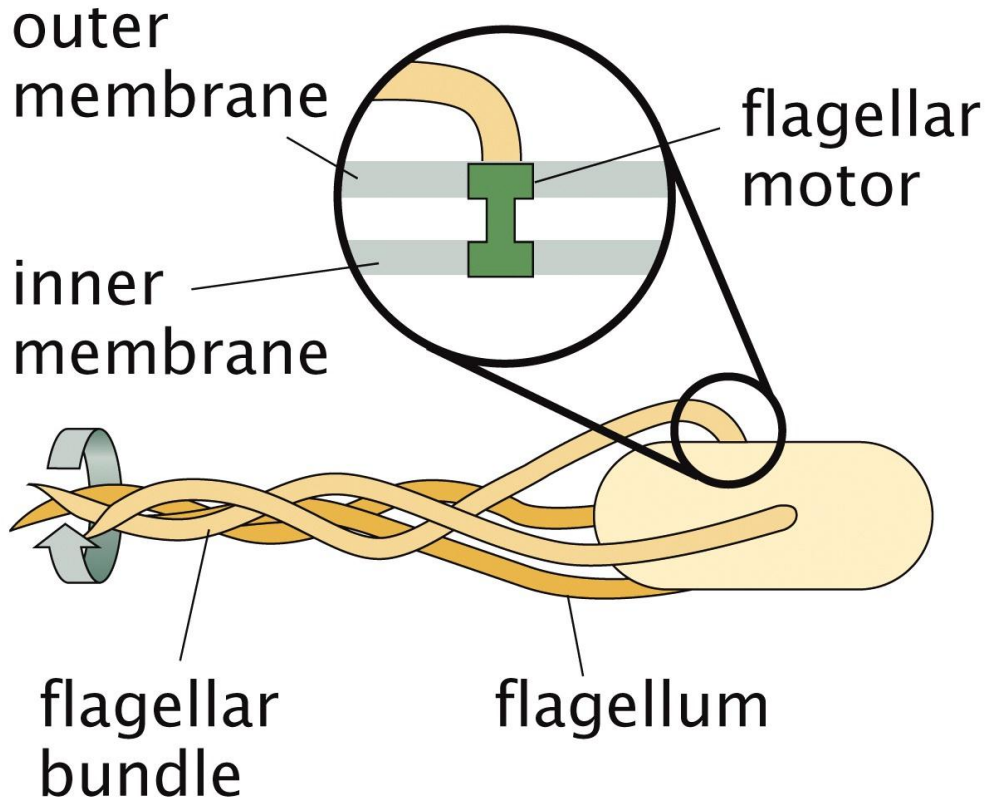
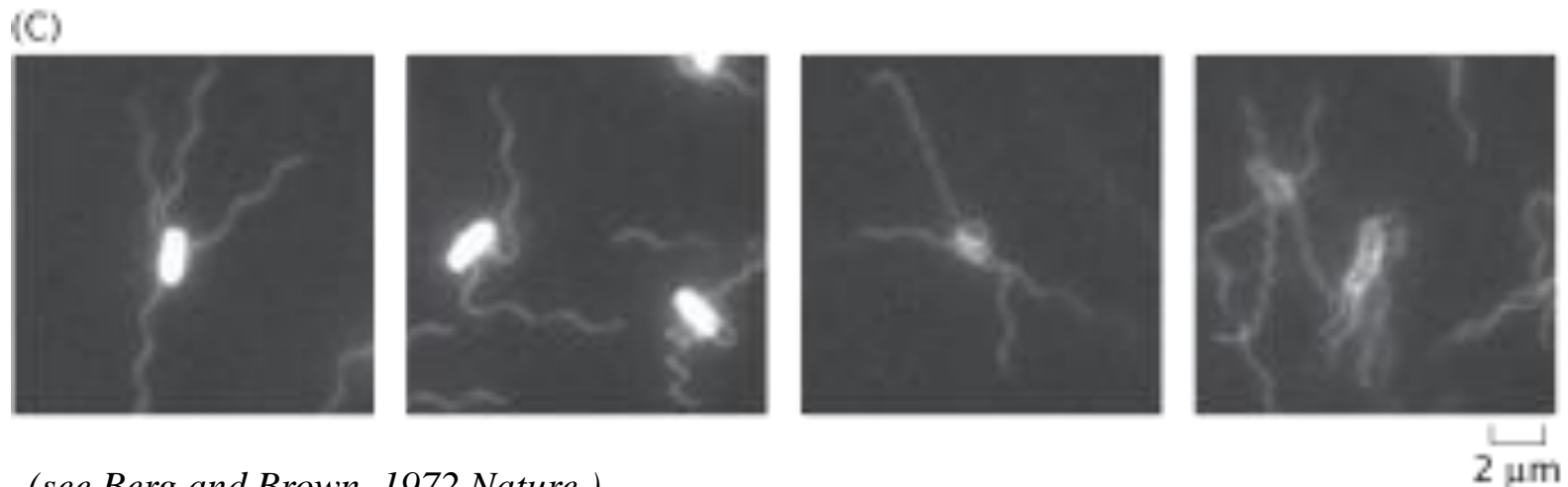
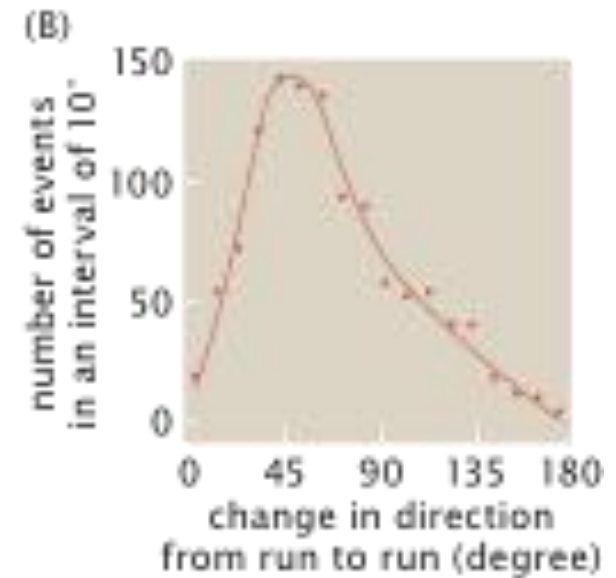
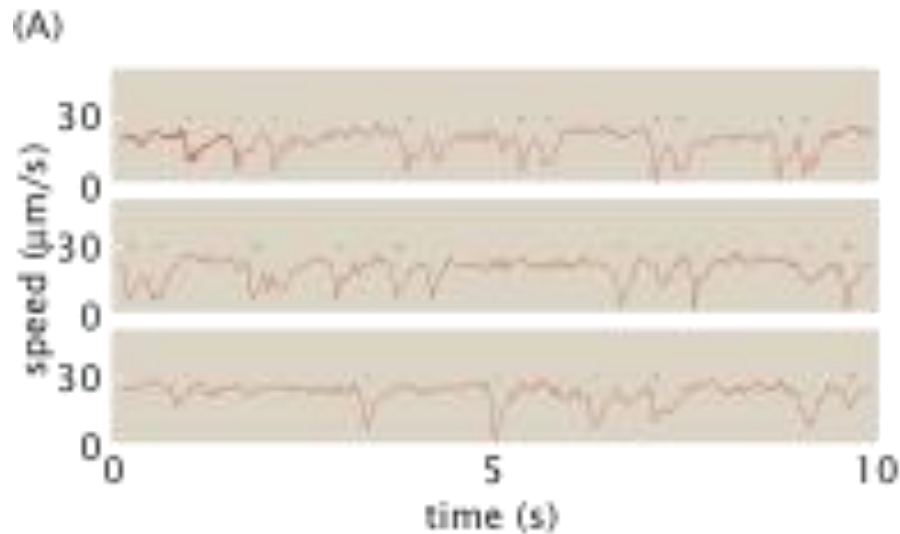


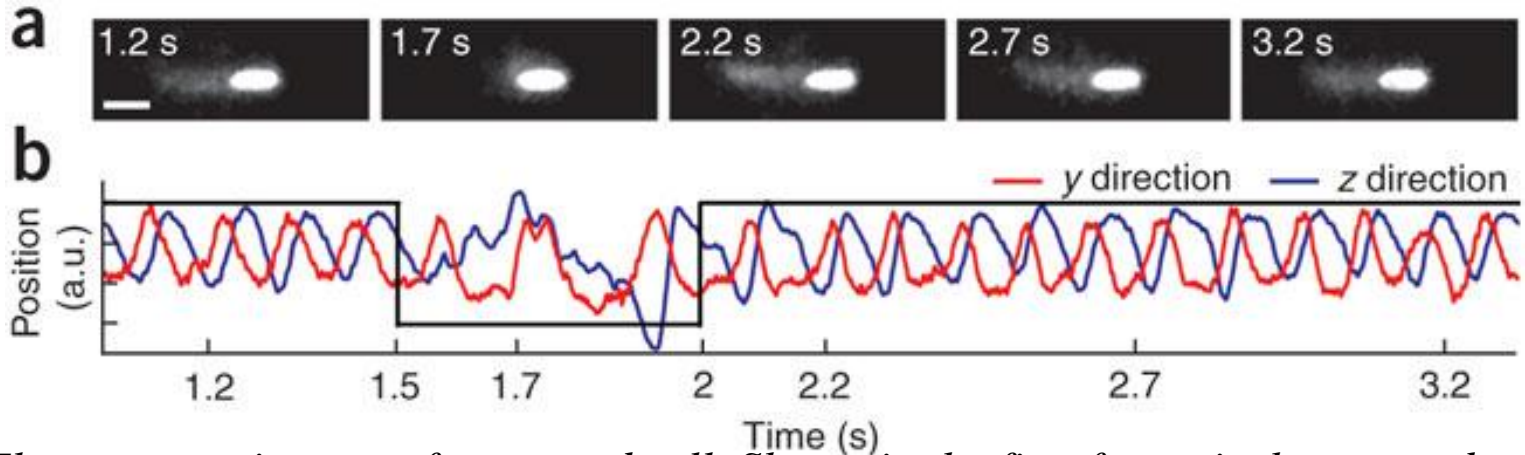
Figure 4.16a Physical Biology of the Cell, 2ed. (© Garland Science 2013)

# Careful measurements by tracking microscopy



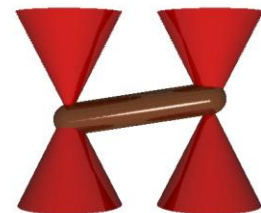
(see Berg and Brown, 1972 Nature.)

# Careful measurements by tracking microscopy



(a) Fluorescence images of a trapped cell. Shown in the first frame is the trapped cell body (bright oval shape) and the flagellar bundle (faint cloud) formed to the left of the cell body. The second frame shows the cell tumbling, with the appearance of a disrupted flagellar bundle. Subsequent frames show the reformed flagellar bundle and the running cell. Each frame was obtained by averaging three successive images collected at a rate of 10 Hz, with the marked time point in the middle. Scale bar, 2  $\mu\text{m}$ . (b) Optical trap signals in the y and z directions, recorded simultaneously with the fluorescence images. Black lines delineate the run (high) and tumble (low) periods. Only the low-frequency component corresponding to body roll is shown for clarity.

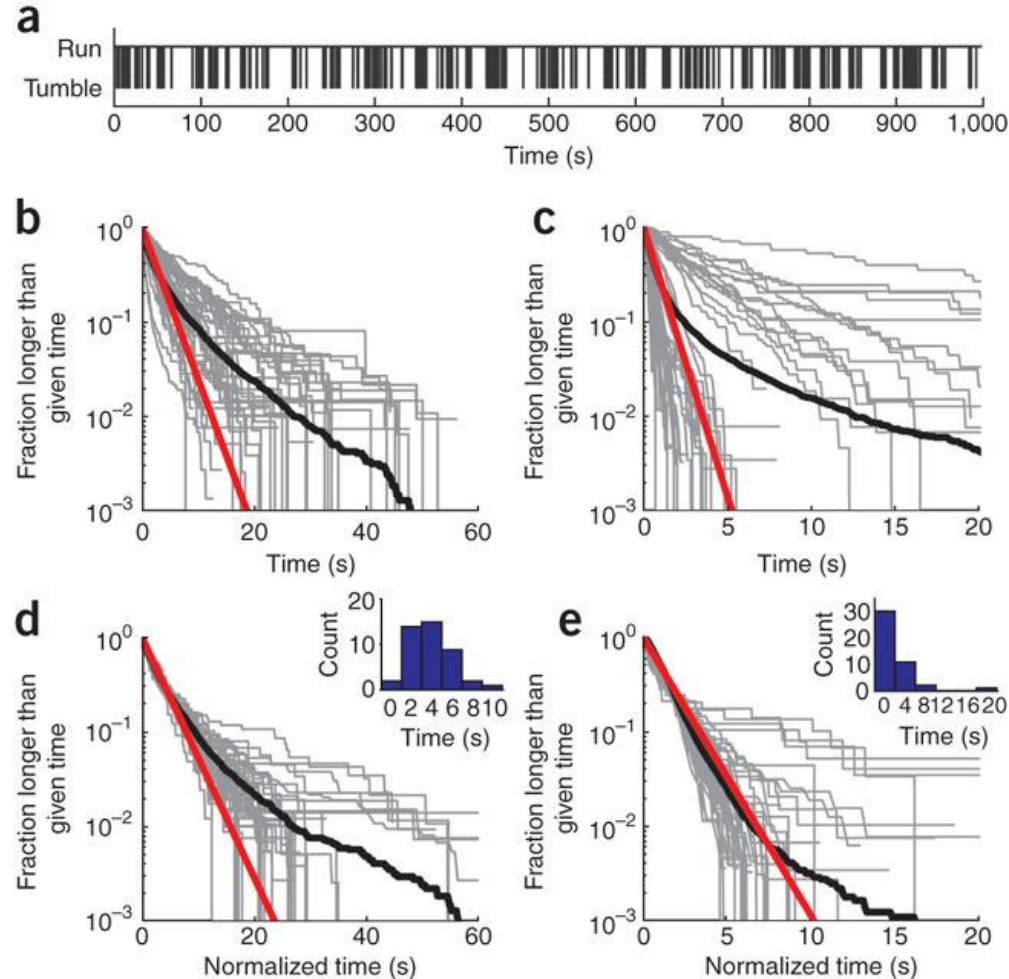
(Chemla, Golding, 2009 Nature Methods.)





# Careful measurements by optical trapping

(a) A typical binary time series generated from the swimming signal of a single trapped cell.  
(b,c) Cumulative distribution of run durations, comprising 5,473 runs observed in 43 wild-type cells (b) and 7,317 runs observed in 44 inducible-bias mutants that showed 20 or more runs (c) (black lines). Each gray line shows the run-time statistics from a single cell. The thick black line is the population ensemble. The red line is an exponential fit to 90% of the data, encompassing the shorter events. Each gray line shows the fraction of runs observed from a single cell that were longer than a given time. The red line is an exponential fit to the first decade of the ensemble distribution. (d,e) Cumulative distribution for wild-type cells (d) and inducible bias mutants (e) in which individual run duration distributions were scaled so that the mean run duration equals the ensemble mean. This scaling procedure collapses data by effectively removing individual variability, thus revealing the underlying universal behavior in the population ensemble. Inset, histogram of mean tumble durations used in scaling.



(see Chemla, Golding et al., 2009 Nature Methods.)

# An amazing molecular machine

- The flagellar motor uses a proton gradient to rotate at roughly the angular speed of a jet engine.
- This motor is a darling of the creationists as an example of something that “couldn’t have evolved” because of its supposed “irreducible complexity”.

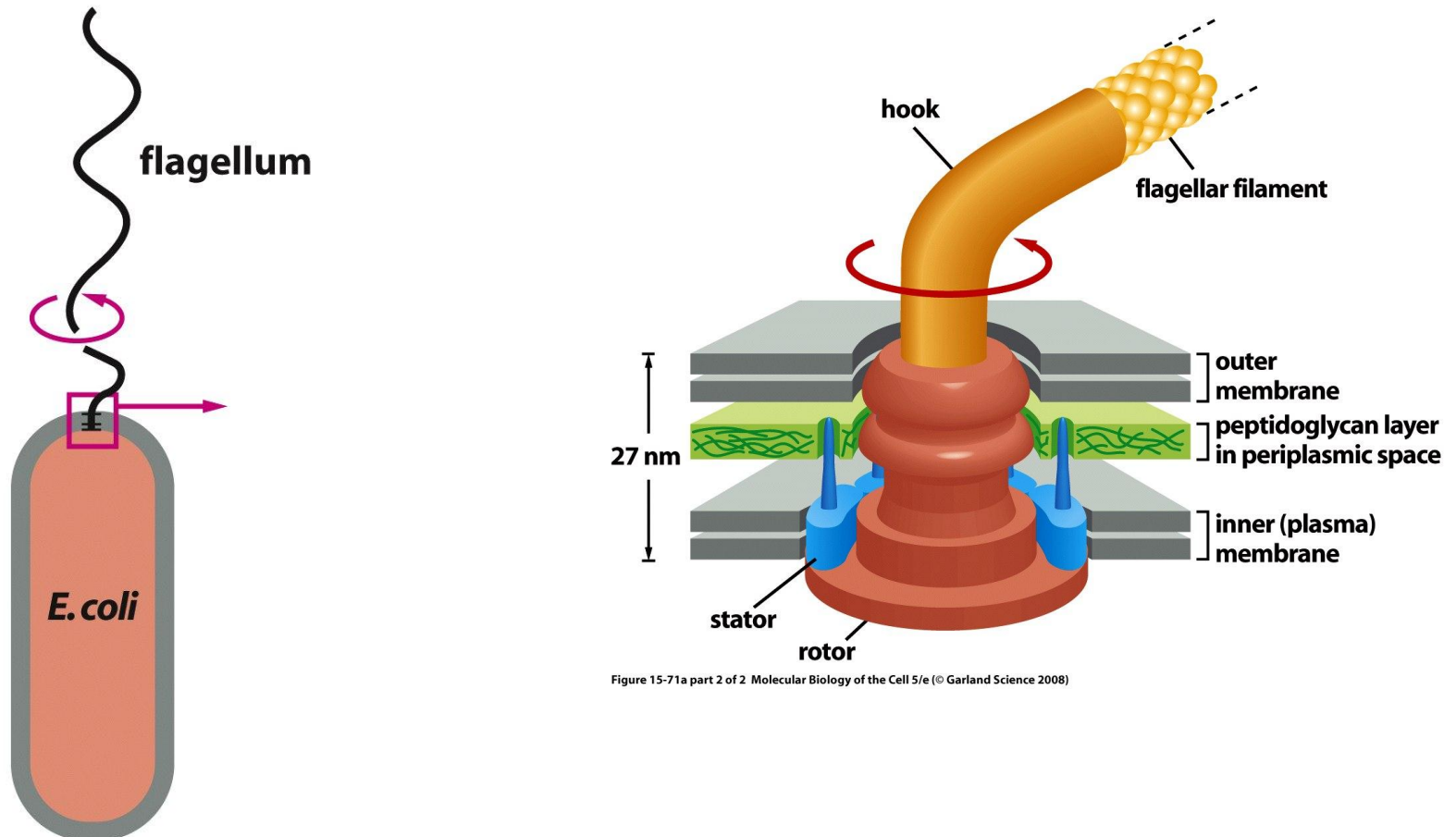


Figure 15-71a part 2 of 2. Molecular Biology of the Cell 5/e (© Garland Science 2008)

Figure 15-71a part 1 of 2. Molecular Biology of the Cell 5/e (© Garland Science 2008)



# Bacterial chemotaxis circuit

- The circuit for bacterial chemotaxis involves precisely the kind of two-component signal transduction system that we discussed earlier.

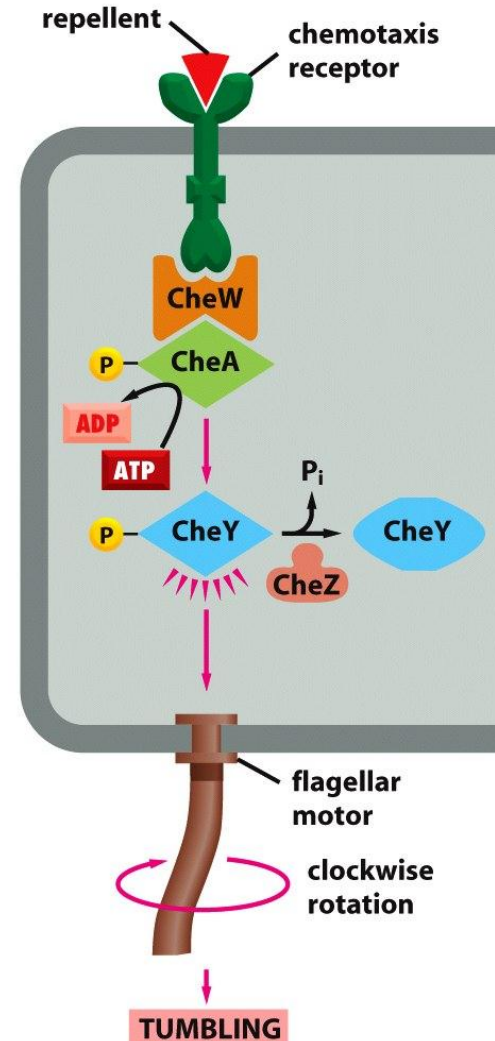


Figure 15-73 Molecular Biology of the Cell 5/e (© Garland Science 2008)

# Nature of the receptors

- Receptors assemble into trimers of dimers.
- Receptor clustering is part of the overall story.

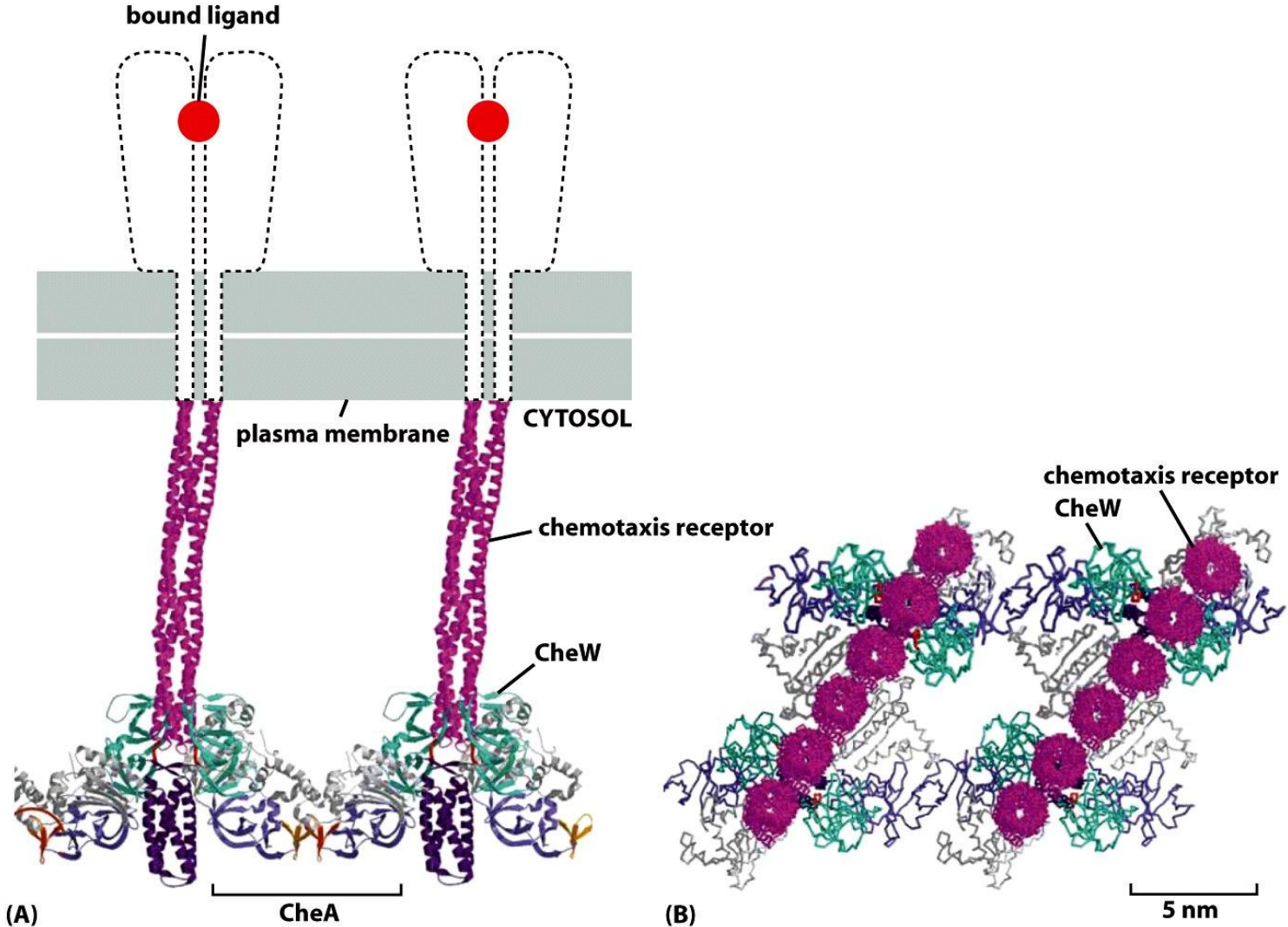
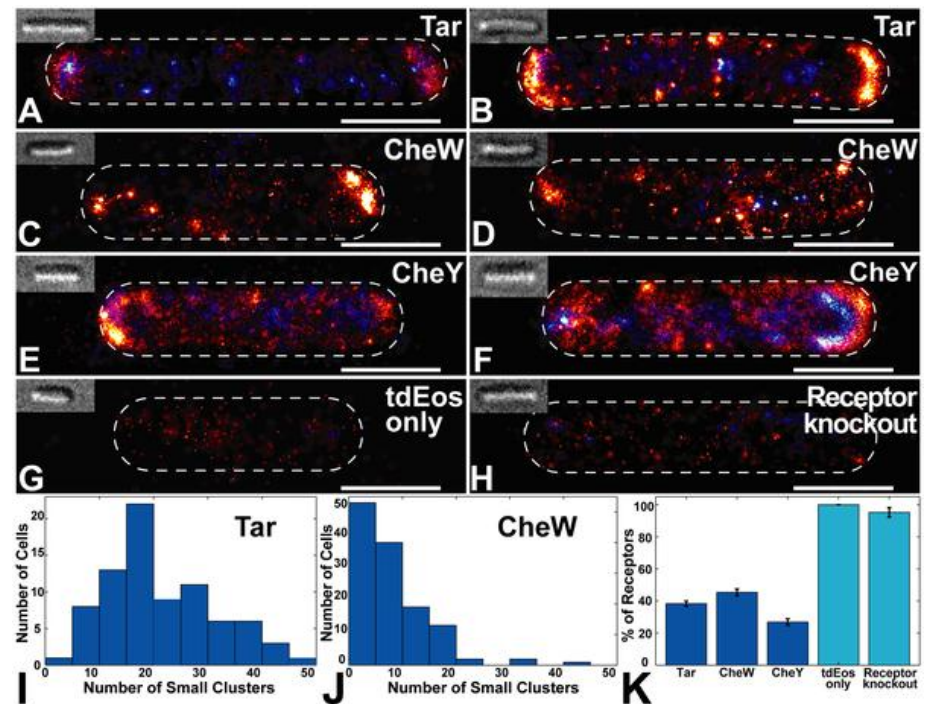
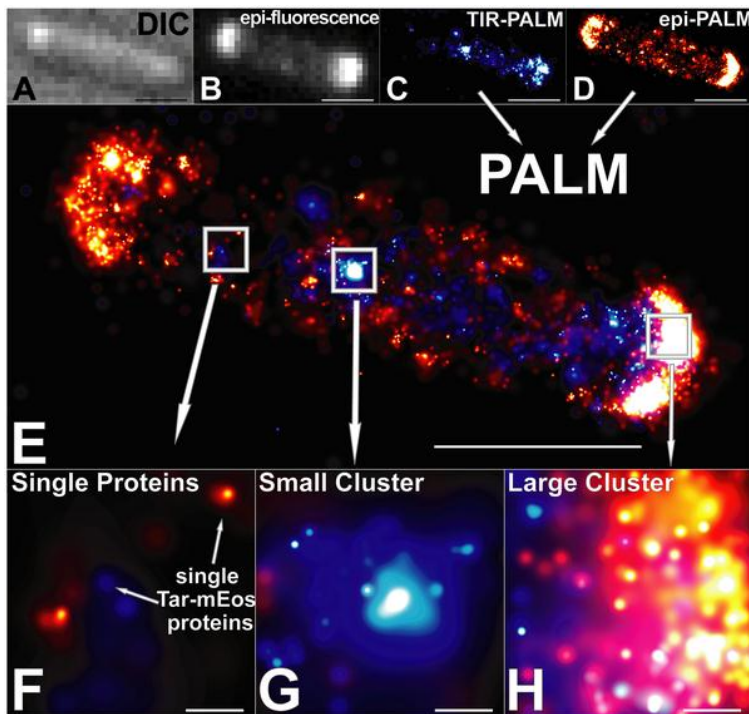


Figure 15-74 Molecular Biology of the Cell 5/e (© Garland Science 2008)

# High resolution imaging of chemotaxis proteins

- PALM is a high-resolution technique that permits beating the diffraction limit.
- In this case, they are looking at chemotaxis proteins in *E. coli*.

(Greenfield, Liphardt et al, PLoS Biology, 2009.)



# Measuring chemotactic activity

- The circuit that mediates chemotaxis is an example of a two-component signal transduction system.
- Study the spatial disposition of the molecular players using FRET.

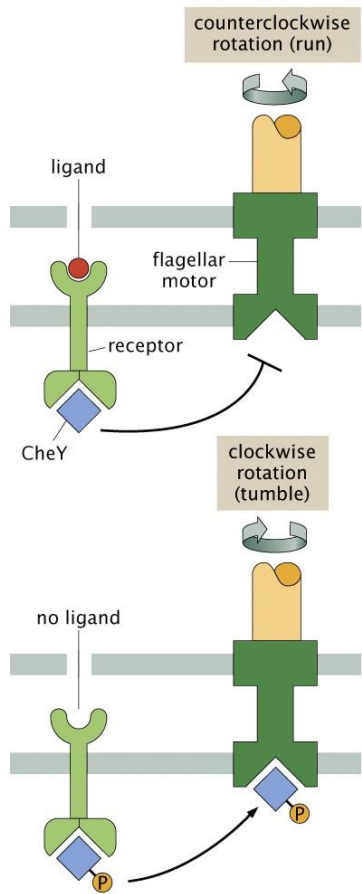


Figure 4.16c Physical Biology of the Cell, 2ed. (© Garland Science 2013)

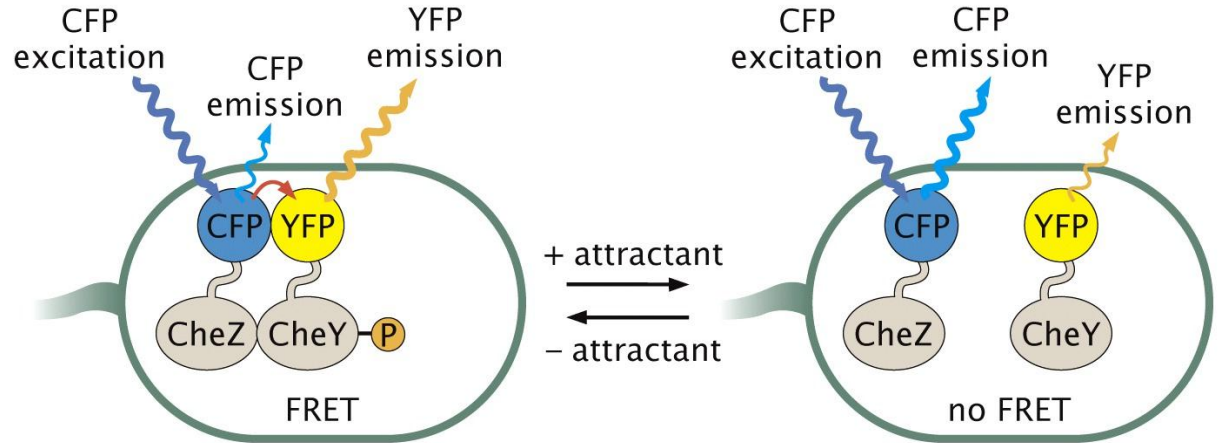


Figure 19.54a Physical Biology of the Cell, 2ed. (© Garland Science 2013)

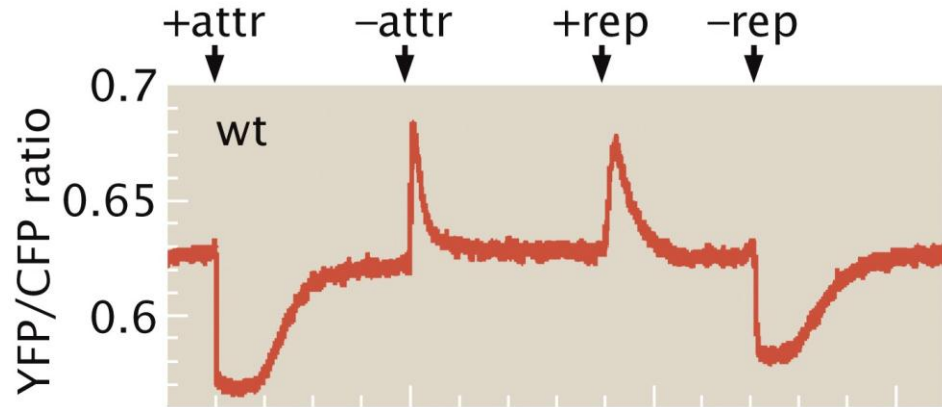


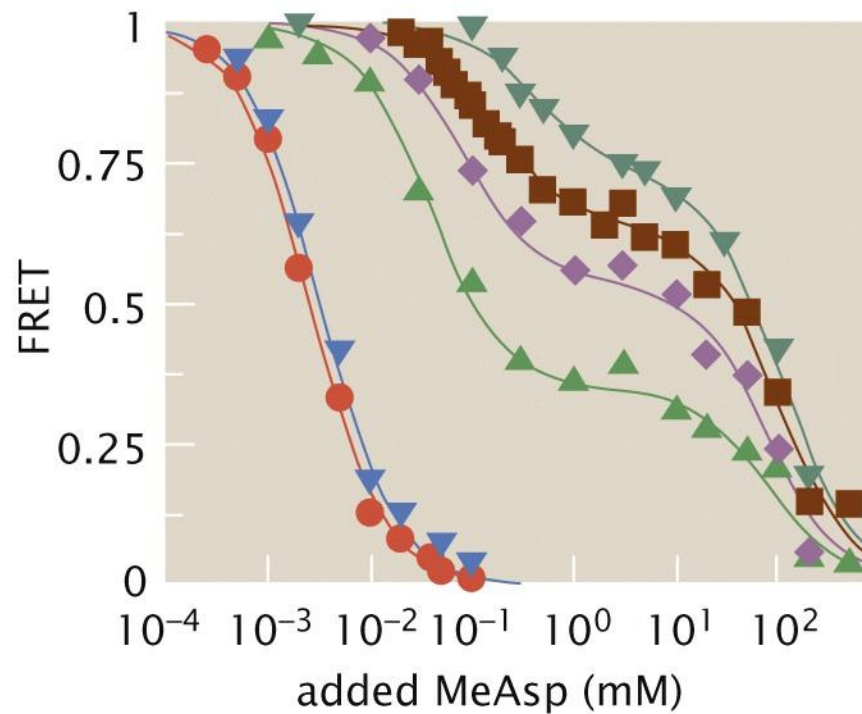
Figure 19.54b Physical Biology of the Cell, 2ed. (© Garland Science 2013)



# The activity curves for different mutants

- The key intuition that we take away from this is that the chemoreceptor is active at low concentrations of chemoattractant and is inactive in the presence of high concentrations of chemoattractant.

(C) experiment



(D) theory

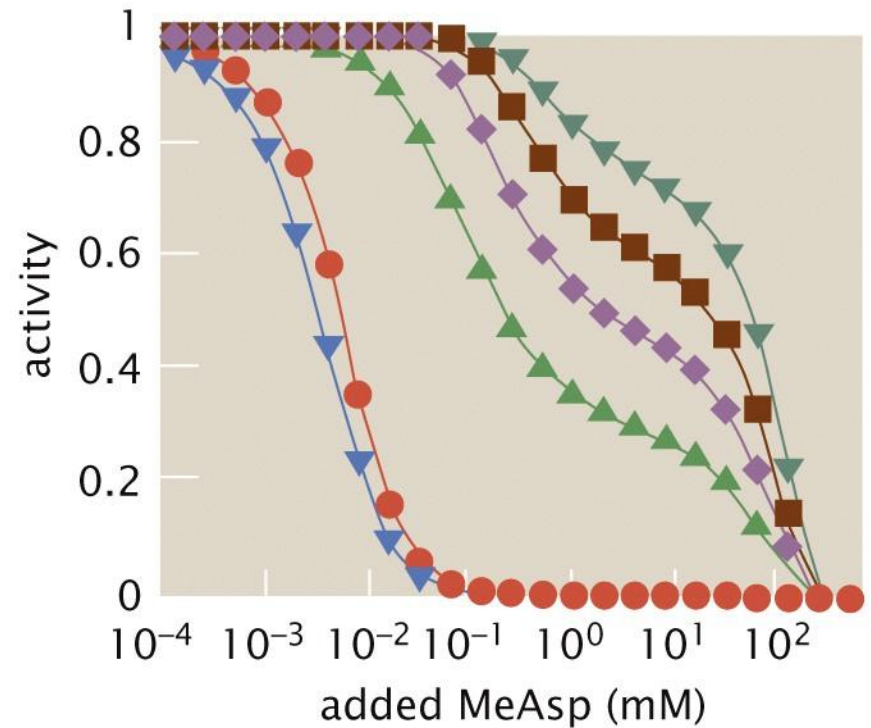
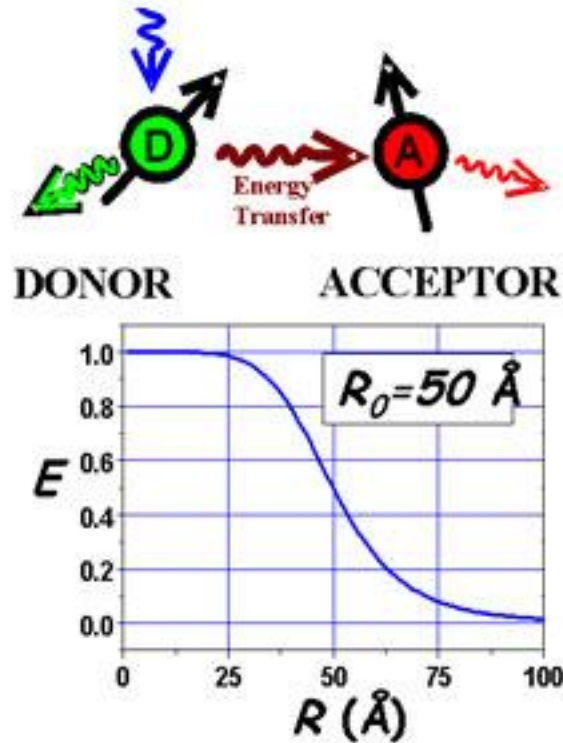


Figure 19.54c Physical Biology of the Cell, 2ed. (© Garland Science 2013)

*J. E. Keymer et al., Proc. Natl Acad. Sci. USA 103:1786, 2006.*

# The fret technique

- Fluorescence resonance energy transfer is an amazing molecular ruler.
- Proximity of acceptor and donor is readout by the efficiency of the transfer.

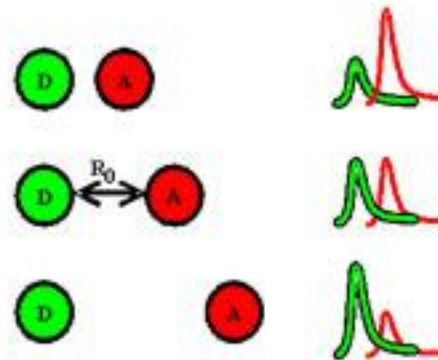


## Energy Transfer Efficiency

$$E = \frac{1}{1 + (R/R_0)^6}$$

$R_0 = 50\%$  transfer efficiency distance  
3nm~7nm

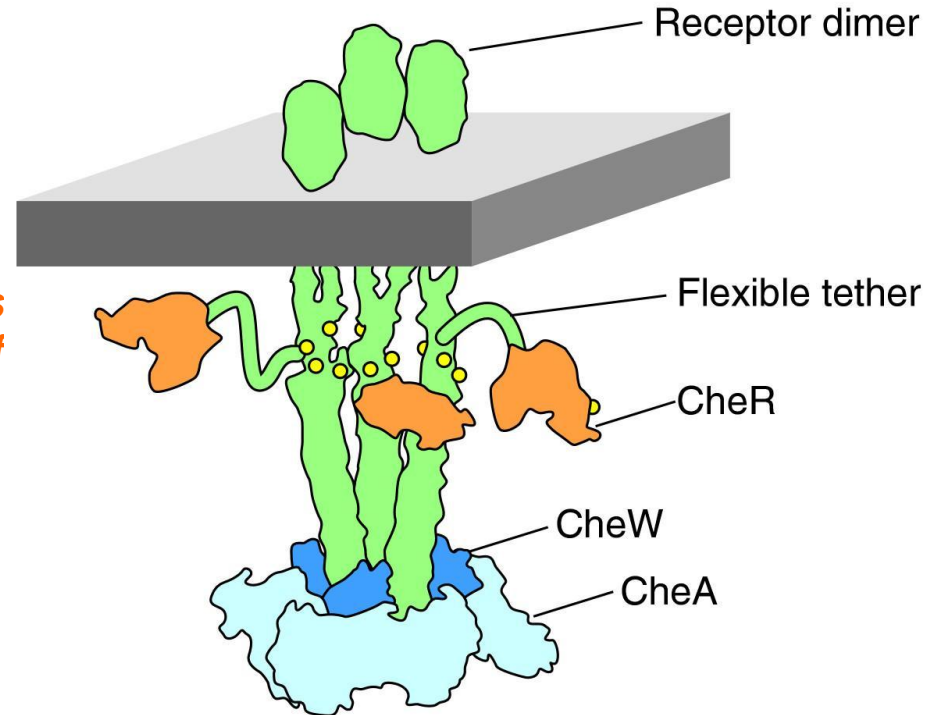
## “Spectroscopic Ruler”



[https://netfiles.uiuc.edu/tjha/www/images/FRET\\_concept.jpg](https://netfiles.uiuc.edu/tjha/www/images/FRET_concept.jpg)

# And the bohr effect reveals itself again

- ◆ The chemoreceptors have methylation sites (shown as yellow circles).
- ◆ Changing the state of methylation has the consequence of altering the equilibrium between active and inactive states and allows the chemoreceptors to adapt to different absolute levels of signal. **NOTE: this is a very common and beautiful feature of biological systems.**
- ◆ Think back to hemoglobin: this is the same basic idea all over again.



$$P_{active}(c) = \frac{\left(1 + \frac{c}{K_d}\right)^n}{\left(1 + \frac{c}{K_d}\right)^n + e^{-\beta\varepsilon} \left(1 + \frac{c}{K_d}\right)^n}$$

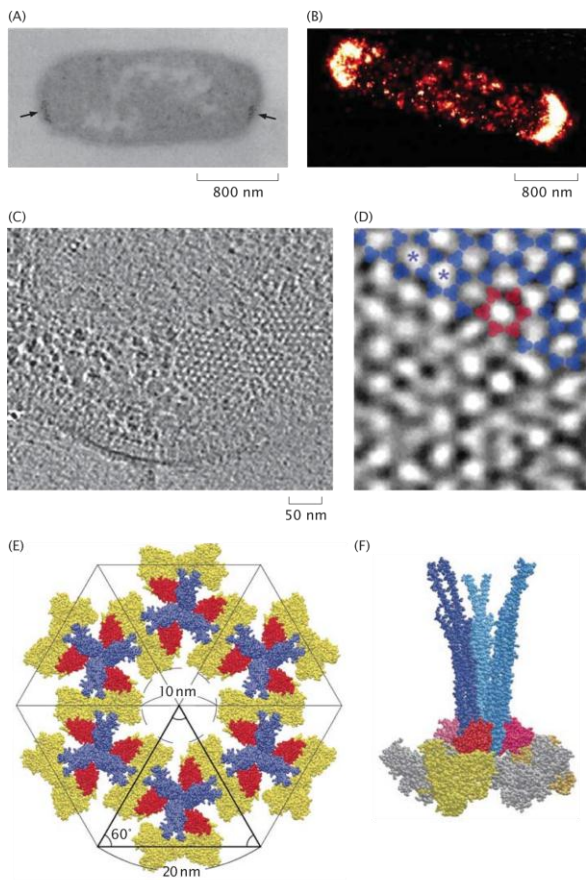
Bohr effect is here



# Key insight: activity curves related to collective behavior of chemoreceptors

Mello and Tu, PNAS 102, 17354 (2005)

Keymer, Endres, Wingreen et al., PNAS 103, 1786 (2006)

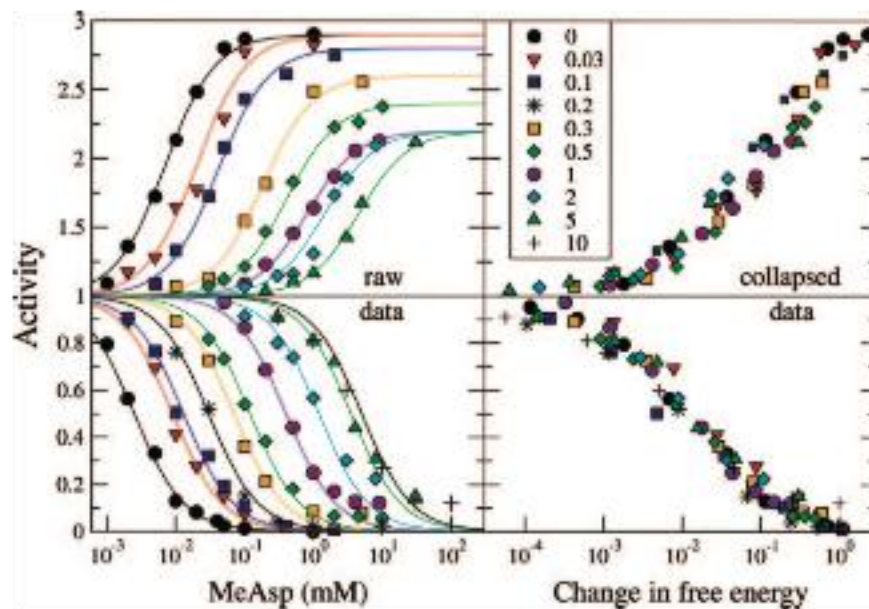


STATE	WEIGHT	DEGENERACY
 N class 1 receptors    M class 2 receptors	$e^{-\beta E_{\text{off}}}$	1
	$e^{-\beta E_{\text{off}}} \frac{c}{K_d^{(1)}(\text{off})}$	N
	$e^{-\beta E_{\text{off}}} \left( \frac{c}{K_d^{(1)}(\text{off})} \right)^2$	$\frac{N(N-1)}{2}$
INACTIVE STATE    ⋮	⋮	⋮
	$e^{-\beta E_{\text{off}}} \left( \frac{c}{K_d^{(2)}(\text{off})} \right)$	M
	$e^{-\beta E_{\text{off}}} \left( \frac{c}{K_d^{(1)}(\text{off})} \right) \left( \frac{c}{K_d^{(2)}(\text{off})} \right)$	N x M
	$e^{-\beta E_{\text{off}}} \left( \frac{c}{K_d^{(1)}(\text{off})} \right)^2 \left( \frac{c}{K_d^{(1)}(\text{off})} \right)^2$	$\frac{N(N-1)}{2} \times M$
⋮	⋮	⋮
SUM ALL OF THESE UP		

ChemotaxisReceptorClusters

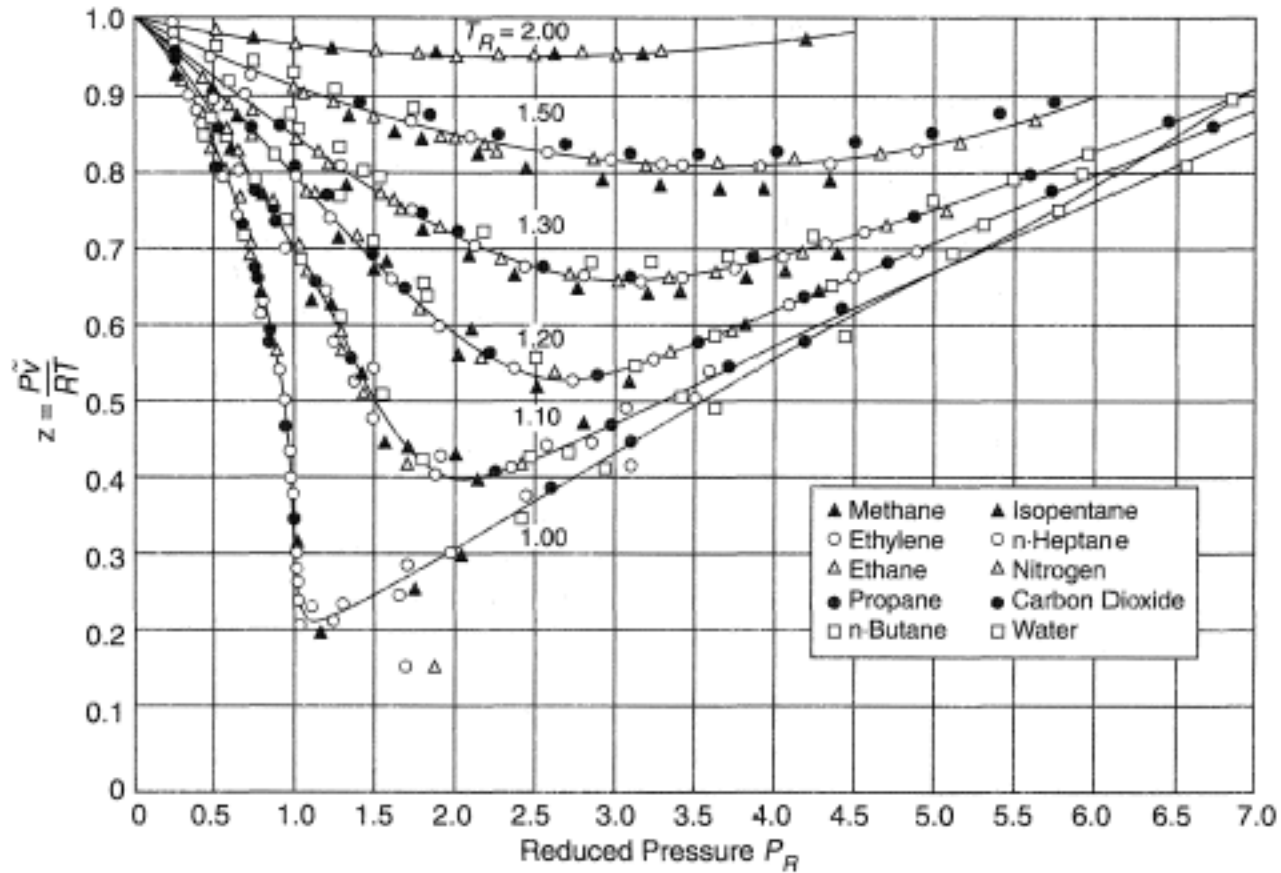
$$p_{\text{active}} = \frac{e^{-\beta E_{\text{on}}} \left( 1 + \frac{c}{K_d^{(1)}(\text{on})} \right)^N \left( 1 + \frac{c}{K_d^{(2)}(\text{on})} \right)^M}{e^{-\beta E_{\text{off}}} \left( 1 + \frac{c}{K_d^{(1)}(\text{off})} \right)^N \left( 1 + \frac{c}{K_d^{(2)}(\text{off})} \right)^M + e^{-\beta E_{\text{on}}} \left( 1 + \frac{c}{K_d^{(1)}(\text{on})} \right)^N \left( 1 + \frac{c}{K_d^{(2)}(\text{on})} \right)^M},$$

# Data collapse tells us about a new parameter: the effective bohr concentration



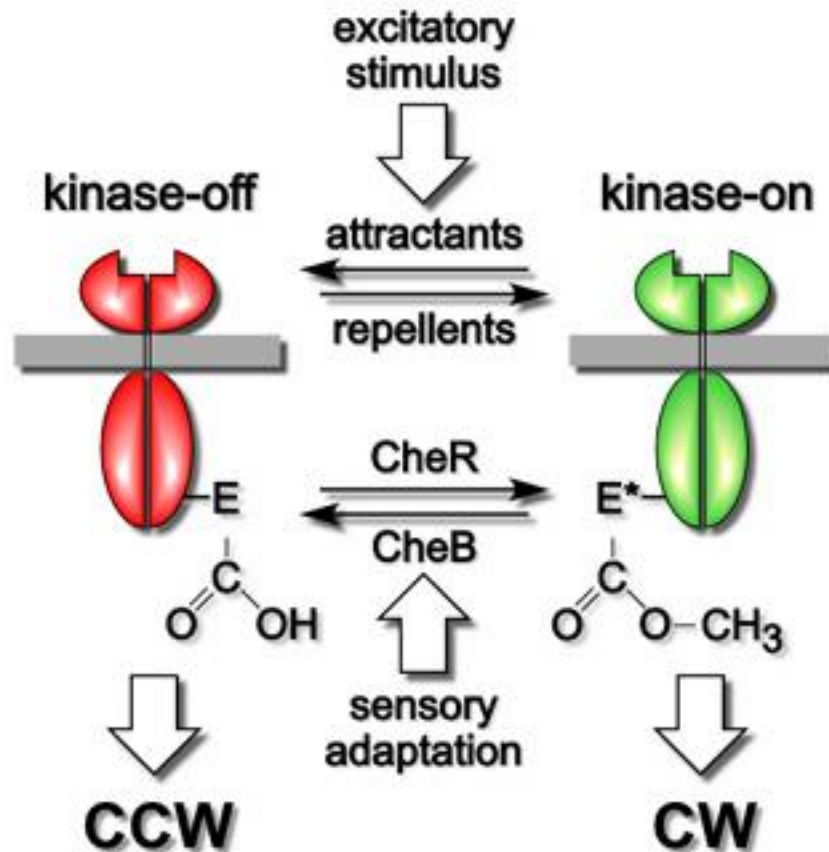
**Fig. 5.** Free-energy scaling of wild-type response. Response measured by FRET to steps of MeAsp in ref. 12 for wild-type adapted cells. (Left) Data are shown for addition (Lower) and subsequent removal (Upper) of MeAsp (with curves to guide the eye) for cells adapted at various ambient MeAsp concentrations (see inset, units are in mM). (Right) Response curves are rescaled according to a free-energy model as described in supporting information. The parameters are the same as in Fig. 1b,  $K_2^{off} = 0.02$  mM,  $K_2^{on} = 0.5$  mM,  $K_2^{off} = 100$  mM.

# Data collapse is often deep: Look up the law of corresponding states

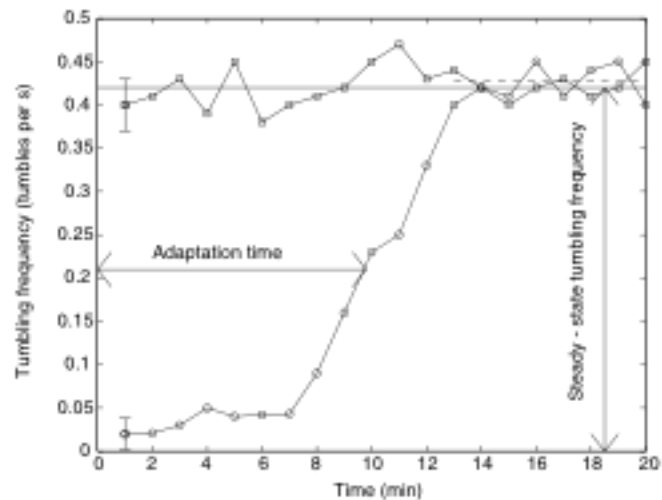


# Adaptation of the circuit

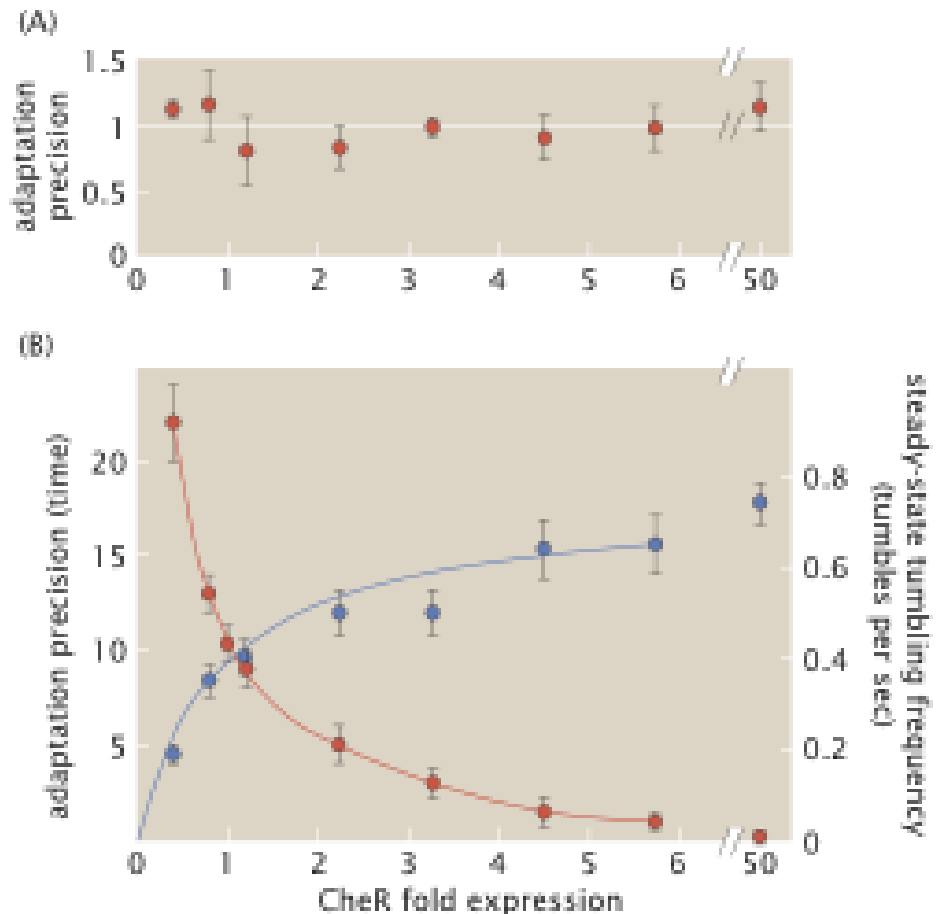
- Methylation provides a scheme for tuning the energy difference between the on and off states of the receptor complex.
- Quantitative measurements leave us with many interesting questions: mutants and their responses, sharpness of response, adaptation, motor binding vs switching, etc...



# Adaptation to chemoattractant

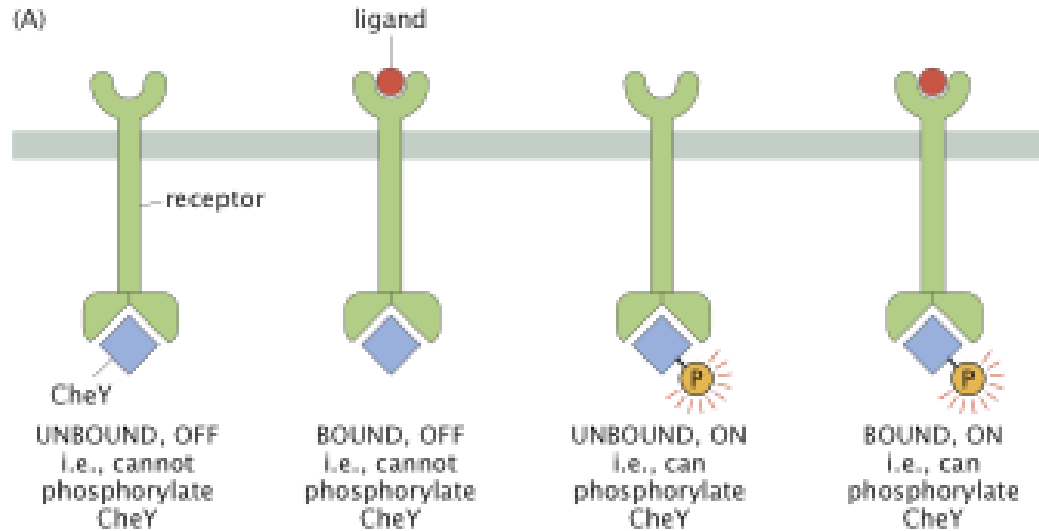


**Figure 1** Tumbling frequency as a function of time for wild-type (RP437) cells. Circles: cells stimulated at time  $t = 0$  by mixing with saturating attractant (1 mM L-aspartate). Squares: unstimulated cells [mock-mixed with chemotaxis buffer]. Tumbling frequency was determined using computerized video tracking<sup>14</sup>. Each point represents data from 10 s motion of 100-400 cells. The adaptation time was defined as the time where the tumbling frequency of stimulated cells rises to halfway between its earliest measured value and its steady-state value. Precision of adaptation was defined as the ratio between the steady-state tumbling frequency of unstimulated cells (full horizontal line) and stimulated cells (dashed horizontal line).



# Building a statistical mechanics model

- Our goal is to find the probability that the receptor will be in the on state as a function of the chemoattractant concentration.


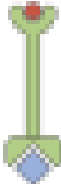
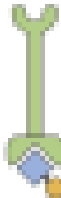



(B)

$$P_{\text{on}} = \frac{\sum \left( \begin{array}{c} \text{Y} \\ | \\ \text{CheY} \end{array} \right) + \sum \left( \begin{array}{c} \text{Y} \\ | \\ \text{CheY} \\ \text{P} \end{array} \right)}{\sum \left( \begin{array}{c} \text{Y} \\ | \\ \text{CheY} \end{array} \right) + \sum \left( \begin{array}{c} \text{Y} \\ | \\ \text{CheY} \\ \text{P} \end{array} \right) + \sum \left( \begin{array}{c} \text{Y} \\ | \\ \text{CheY} \\ \text{P} \end{array} \right) + \sum \left( \begin{array}{c} \text{Y} \\ | \\ \text{CheY} \\ \text{P} \end{array} \right)}$$

# States and weights

- Each of the states has a corresponding statistical weight.

STATE	WEIGHT
	$\frac{\Omega!}{L(\Omega-L)!} e^{-\beta \epsilon_{\text{set}}} e^{-\beta \epsilon_{\text{off}}}$
	$\frac{\Omega!}{(L-1)(\Omega-(L-1))!} e^{-\beta(L-1)\epsilon_{\text{set}}} e^{-\beta \epsilon_{\text{off}}} e^{-\beta \epsilon_b^{\text{off}}}$
	$\frac{\Omega!}{L(\Omega-L)!} e^{-\beta \epsilon_{\text{set}}} e^{-\beta \epsilon_{\text{on}}}$
	$\frac{\Omega!}{(L-1)(\Omega-(L-1))!} e^{-\beta(L-1)\epsilon_{\text{set}}} e^{-\beta \epsilon_{\text{on}}} e^{-\beta \epsilon_b^{\text{on}}}$



# MWC model for receptor activity

- MWC model of chemoreceptor activity.

